Medicated Janus fibers fabricated using a Teflon-coated side-by-side spinneret

Bligh, SWA., Yu, Deng-G., Shen, Chen-Y., Jin, M., Williams, Gareth R., Zou, H. and Wang, X.

Medicated Janus fibers fabricated using a Teflon-coated side-by-side spinneret

Deng-Guang Yu [a,*], Chen Yang [a], Miao Jin [b], Gareth R. Williams [b], Hua Zou [a], Xia Wang [a,**], SW Annie Bligh [c,***]

[a] School of Materials Science & Engineering, University of Shanghai for Science and Technology, Shanghai 200093, China.
[b] UCL School of Pharmacy, University College London, London WC1N 1AX, UK.
[c] Faculty of Science and Technology, University of Westminster, 115 New Cavendish Street, London W1W 6UW, UK.

*** Corresponding authors:**
Prof. Deng-Guang, Prof. SW Annie Bligh and Prof. Xia Wang

Address:
School of Materials Science & Engineering,
University of Shanghai for Science and Technology,
516 Jungong Road, Yangpu District,
Shanghai 200093, P.R. China
Tel: +86-21-55270632
Fax: +86-21-55270632
Email: ydg017@usst.edu.cn; a.bligh@westminster.ac.uk; wangxia@usst.edu.cn

ABSTRACT:

A family of medicated Janus fibers that provides highly tunable biphasic drug release was fabricated using a side-by-side electrospinning process employing a Teflon-coated parallel spinneret. The coated spinneret facilitated the formation of a Janus Taylor cone and in turn high quality integrated Janus structures, which could not be reliably obtained without the Teflon coating. The fibers prepared had one side consisting of polyvinylpyrrolidone (PVP) K60 and ketoprofen, and the other of ethyl cellulose (EC) and ketoprofen. To modulate and tune drug release, PVP K10 was doped into the EC side in some cases. The fibers were linear and had flat morphologies with an indent in the center. They provide biphasic drug release, with the PVP K60 side dissolving very rapidly to deliver a loading dose of the active ingredient, and the EC side resulting in sustained release of the remaining ketoprofen. The addition of PVP K10 to the EC side was able to accelerate the second stage of release; variation in the dopant amount permitted the release rate and extent this phase to be precisely tuned. These results offer the potential to rationally design systems with highly controllable drug release profiles, which can complement natural biological rhythms and deliver maximum therapeutic effects.

KEYWORDS: Janus fibers; side-by-side electrospinning; Teflon-coated spinneret; nano drug delivery systems; tunable release rates; structural nanocomposites

1. Introduction

A range of "top-down" nanofabrication techniques exists, but of these electrohydrodynamic atomization (EHDA, including electrospinning, electrospraying and e-jet printing) is particularly attractive because of its simplicity and capability to propagate the structure of a macroscale template into a nanostructure [1,2]. An EHDA process typically involves preparing a solution of a polymer (possibly also with a functional component) in a volatile solvent. This solution is then ejected at a precisely controlled rate from a syringe fitted with a metal needle (spinneret) towards a grounded collector plate [3-7]. A large potential difference is applied between the spinneret and collector plate. This electrical energy causes very rapid evaporation of the solvent, leading to a solid product. The spatial distribution of components in the latter mirrors that in the spinneret.

Considering a two-compartment system, the simplest structures are i) core-shell (with different interior and exterior) and ii) an asymmetric Janus structure, where the sides of the structure are different. Both can be used to develop materials with tunable or multifunctional properties. Core-shell structures, including fibers and particles, generated by EHDA have been widely explored [8,9]. These are most commonly fabricated from a concentric spinneret [10,11], although they can also be prepared using a single fluid process [12,13]. More complex structures such as three-layer nanofibers and microparticles (from tri-axial EHDA processes) and multi-compartmental structures from multiple fluid spinnerets have also been reported [14,15]. However, there are very few publications reporting electrospun Janus fibers,

although there are hundreds on electrospun core-shell nanofibers. .

Unlike core/shell architectures the Janus structure permits direct contact of both compartments with their environment, which are very useful for creating multi-functional nanoproducts [16]. Such structure types are also commonly found in nature [17], and Janus nanoparticles are currently one of the most high profile topics in the nano field [18,19]. Since Gupta and Wilkes first reported the fabrication of Janus fibers using side-by-side electrospinning with polyvinyl chloride/polyurethane and polyvinyl chloride)/polyvinylidiene fluoride [20], only a very limited number of additional studies have followed their initial work [21-23]. This can be attributed to the difficulty of creating integrated Janus nanostructures when parallel metal capillaries are used as a spinneret for side-by-side electrospinning.

Biphasic controlled release of an active ingredient is much sought after in pharmaceutics, particularly with an initial rapid release stage followed by sustained release. Drug delivery systems (DDS) providing such release profiles can deliver an effective “loading dose”, producing a rapid rise in the plasma concentration of drug and rapidly relieving a patient’s symptoms. Subsequently, a prolonged-release phase maintains an effective therapeutic concentration, avoiding repeated administrations [24].

Different types of biphasic release DDS for potential oral administration have been reported, fabricated using a wide variety of technologies [25]. Biphasic release fibers from single fluid electrospinning have been generated through the encapsulation of nanoparticles in the fibers [26] or the collection of different types of fibers in a

layer-by-layer manner [27]. However, the former method involved a complex multiple-step preparation process, and the layer-by-layer collection of different fibers often resulted in non-homogeneous products. Coaxial electrospinning can yield biphasic release DDS in a single step, as a result of its ability to produce materials where the composition of the core and shell are different [24,25]. By changing the shell-to-core fluid flow rate ratio [24] or the concentration of drug in the working fluids [28], a tunable biphasic release profile with accurate control of the amount of drug released in the different phases can be realized.

However, to date there are no reports describing the tuning of the release rate in the sustained phase of release in an electrospun biphasic DDS. Being able to precisely control the rate of sustained release is important to ensure the most effective and safe pharmacokinetic profile for a particular disease, and to facilitate maximum absorbance of the drug after oral administration. For many drugs, absorption is moderately slow in the stomach, rapid in the proximal intestine, and declines sharply in the distal segment of the intestine [29].

In this work, we aimed to develop a new side-by-side electrospinning process for creating integrated Janus fibers. A new Teflon-coated spinneret was exploited to ensure the two working fluids converge before they were ejected from the spinneret. A series of ketoprofen-loaded Janus fibers has been prepared using poly(vinylpyrrolidone) (PVP) K60 and ethyl cellulose (EC). The fibers exhibit biphasic drug release, with an initial burst release followed by sustained freeing of drug into solution. The release rate and extent in the second phase can be tuned by doping small amounts of PVP K10 into

the EC side of the fiber systems. As a result, nanoscale drug delivery systems with highly tunable release profiles have been produced; these cannot easily be achieved using traditional pharmaceutical technologies, and thus this work offers the potential to lead to a range of new medicines and concomitant patient benefit.

2. Experimental

2.1. Materials

Polyvinylpyrrolidone K60 (PVP K60, M_w=360,000) and PVP K10 (M_w=10,000) were purchased from Sigma-Aldrich Ltd. (Shanghai, China). Ethyl cellulose (EC, 6mPa·s to 9 mPa·s) was obtained from the Aladdin Chemistry Co. Ltd. (Shanghai, China). Keteprofen (KET) was purchased from the Wuhan Fortuna Chemical Co. Ltd. (Hubei, China). Methylene blue and anhydrous ethanol were obtained from the Sinopharm Chemical Reagent Co. Ltd. (Shanghai, China). All other chemicals used were analytical grade. Water was doubly distilled immediately prior to use.

2.2. Side-by-side electrospinning

After initial optimization experiments, the solutions used for electrospinning consisted of (1) 8% (w/v) PVP K60 and 2% (w/v) KET in ethanol, and (2) 24% (w/v) EC, 2% (w/v) KET and a varied content of PVP K10 (0, 1, 2, and 5% (w/v)) in ethanol.

Two homemade side-by-side spinnerets were used for electrospinning. A flat piece of cardboard covered with aluminum foil was earthed and used as the collector plate. Two syringe pumps (KDS100 and KDS200, Cole-Parmer®, Vernon Hills, IL, USA) were used to drive the working fluids. A ZGF 60kV/2mA power supply (Shanghai Sute Corp., Shanghai, China) was employed to provide a potential

153 difference between the spinneret and collector.

154 Electrospinning was conducted under ambient conditions (24 ± 2 °C with a
155 relative humidity of 51 ± 7 %). After optimization, the applied voltage was fixed at 12
156 kV, the fiber to collector distance at 20 cm and the flow rates of both the PVP K60 and
157 EC solutions set to 1.0 mL/h. The electrospinning processes were recorded using a
158 digital video recorder (PowerShot A490, Canon, Tokyo, Japan).

159 **2.3. Characterization**

160 *2.3.1. Morphology and structure*

161 The morphologies of the fiber products were investigated using a Quanta FEG450
162 field-emission scanning electron microscope (FESEM, FEI Corporation, Hillsboro,
163 USA). The samples were subjected to gold sputter-coating in a nitrogen atmosphere
164 prior to imaging. Average sizes (diameters for monolithic nanofibers and widths for
165 Janus fibers) were determined by measuring the fibers at more than 100 different
166 places in FESEM images, using the Image J software (National Institutes of Health,
167 Bethesda, USA).

168 The fiber structures were also studied on a JEM 2100F field-emission
169 transmission electron microscope (TEM, JEOL, Tokyo, Japan). TEM samples were
170 prepared by placing a lacey carbon-coated copper grid on the fiber collector and
171 electrospinning onto it for several minutes.

172 *2.3.2. Functional performance*

173 *In vitro* dissolution tests were conducted according to the Chinese Pharmacopoeia
174 (2015 ed.) Method II, a paddle method. Experiments were undertaken using a RCZ-8A

dissolution apparatus (Tianjin University Radio Factory, Tianjin, China).

A mass of fibers containing 40 mg KET (200, 519, 360, 370, 381 and 408 mg for fibers F1, F2, F3, F4, F5 and F6, respectively) was placed in 800 mL physiological saline (PS, 0.9% wt) at 37 ± 1 °C, providing sink conditions with $C < 0.2C_s$. The dissolution vessels were stirred at 50 rpm. At predetermined time points, 5.0 mL aliquots were withdrawn from the dissolution medium and replaced with fresh PS to maintain a constant volume. After filtration through a 0.22 μm membrane (Millipore, Billerica, USA) and appreciate dilution with PS, the samples were analyzed at λ_{max} = 260 nm using a UV-vis spectrophotometer (UV-2102PC, Unico Instrument Co. Ltd., Shanghai, China). The accumulative KET released was back-calculated from the data obtained against a predetermined calibration curve. All experiments were repeated six times, and results given as mean ± S.D.

3. Results and discussion

3.1. Implementation of the side-by-side electrospionning

Traditionally, a side-by-side spinneret comprises two parallel metal capillaries. Here, we used a section of Teflon tube to coat the parallel metal capillaries on their outlets and project slightly over their nozzles (see the Supplementary Information, Fig. S1). The Teflon coating has several advantages: 1) it can effectively prevent the separation of the two working fluids that occurs when a traditional parallel spinneret is used; 2) an even distribution of charge around the spinneret is expected to be achieved; 3) because Teflon is non-conductive, all the charge from the power supply can be directed effectively to the working fluids [25]; 4) the non-stick nature of Teflon

will mean that fibers should not stick to the spinneret, and thus clogging can be avoided. These factors should all facilitate the formation of a Janus Taylor cone [30].

Table 1. Details of the electrospinning processes and resultant products.

No.	Process	PVP K60 side [a]	EC side				Size [b] (μm)	P [c] (%)
		Flow rate (mL/h)	Flow rate (mL/h)	Composition (% w/v)				
				EC	KET	PVP K10		
F1	Single	1.0	--		--		0.57±0.09	20
F2	Single	--	1.0	24	2	0	0.68±0.13	7.7
F3	Side-by-side	1.0	1.0	24	2	0	0.92±0.10	11.1
F4	Side-by-side	1.0	1.0	24	2	1	1.02±0.17	10.8
F5	Side-by-side	1.0	1.0	24	2	2	0.98±0.13	10.5
F6	Side-by-side	1.0	1.0	24	2	5	1.06±0.12	9.8

[a] This fluid consisted of PVP K60 (8% w/v) and KET (2% w/v)

[b] Values are shown as mean ± S.D. For F1 and F2, ''size'' refers the fiber diameter, and for F3 to F6 to the full width of the combined Janus fibers.

[c] P is the total drug content in the solid fibers calculated according to the flow rate and drug content in the fluids: $P = [(F_p \times C_{pd}) + (F_e \times C_{ed})]/[(F_p \times C_{pa}) + (F_e \times C_{ea})] \times 100\%$. F_p and F_e are the flow rates of the PVP side and EC side, respectively; C_{pd} and C_{ed} the drug contents in PVP and EC sides; and C_{pa} and C_{ea} the total solute content in the PVP and EC solutions.

In this study six different fibers, two monolithic and four Janus, were prepared. Details of the electrospinning processes are given in Table 1. The apparatus deployed for side-by-side electrospinning is shown in Fig. 1a. The Teflon-coated spinneret was mounted on a polypropylene syringe containing a PVP K60 solution. The syringe was then placed vertically above the collector. A second syringe containing an EC solution was connected to the second capillary of the spinneret *via* a flexible silicone tube. For easy observation of the electrospinning processes, 0.001% (w/v) of methylene blue was added to the EC solution.

After a series of optimization experiments, a stable electrospinning process was achieved, as depicted in Fig. 1b. A straight fluid jet was emitted from a Janus Taylor

cone (Fig. 1c), followed by an unstable region of bending and whipping with coils of increasing size. The resultant fiber mat was light blue, with an even blue hue across the product. This was attributed to the presence of methylene blue; the homogeneous color distribution is indicative of an integrated Janus structure.

In contrast, when the process was performed without the Teflon coating the fiber mat had an uneven blue color (Fig. 1d), demonstrating a failure to generate integrated and homogeneous structures. The two fluids used for electrospinning were observed to separate from one other immediately upon exiting the spinneret (Fig. 1e). When two fluids are ejected from the nozzles of a side-by-side spinneret, there is only a very small contact area between them. Since they originate in different capillaries, both fluids will be charged prior to coming into contact and thus it is inevitable that they will repel one another, preventing them from converging to form a Janus Taylor cone; this is illustrated in Fig. 1f(A). This initial repulsive force, F_t, leads to two Taylor cones; it is then followed by further repulsion between the two straight fluid jets (F_s) and the two bending and whipping coils (F_c). These factors result in the failure to form integrated Janus structures. When the spinneret was coated with Teflon (Fig. 1f(B)), the two fluids are found to first converge, before forming a compound Taylor cone and ultimately resulting in integrated Janus structures.

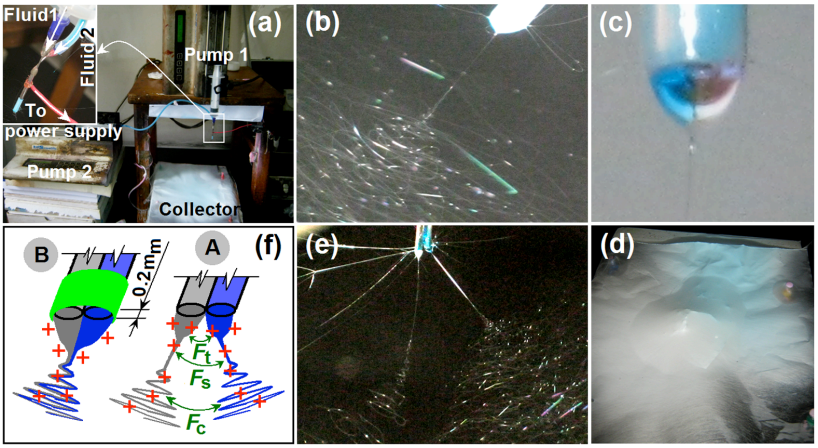

Fig. 1. The side-by-side electrospinning process: (a) The experimental apparatus (inset: the connection of the side-by-side spinneret with the working fluids and power supply); (b) a photograph of a typical side-by-side electrospinning process with the Teflon-coated spinneret; (c) a Janus Taylor cone formed with the Teflon-coated spinneret; (d) The fiber mat from side-by-side electrospinning with the uncoated side-by-side spinneret; (e) the separation of fluids when using the uncoated spinneret; (f) an illustration of the role played by the Teflon coating: A - the separation of fluids arising from repulsive forces F_t (between the two Taylor cones), F_s (between the two straight fluid jets) and F_c (between the two coils); and B - the formation of an integrated Janus Taylor cone with the Teflon coating.

3.2. Morphologies and structures of the fabricated Janus nanofibers

First, the monolithic fibers F1 and F2 were prepared by single fluid electrospinning using the traditional side-by-side spinneret with one fluid turned off. Both fluids individually were found to have good electrospinnability. FESEM images of F1 (PVP K60 and KET) are shown in Fig. 2a. The fibers have a linear morphology and smooth surfaces, and an average diameter of 0.57 ± 0.09 μm. The FESEM images

of F2 (EC and KET) are depicted in Fig. 2b; again the fibers are smooth and linear, possessing an average diameter of 0.68 ± 0.13 μm.

The FESEM images of the Janus fibers F3, F4, F5 and F6 are exhibited in Fig. 2c to Fig 2f. All have linear morphologies and smooth surfaces. While the monolithic fibers are cylindrical in shape, these fibers have a flat concave topography but are still linear and smooth. The two sides of the fibers can clearly be resolved. The fiber diameters can be found in Table 1. F4 to F6 contain small amounts of PVP K10 doped into the EC side of the fibers, but this is found to have no significant influence on their size or morphology.

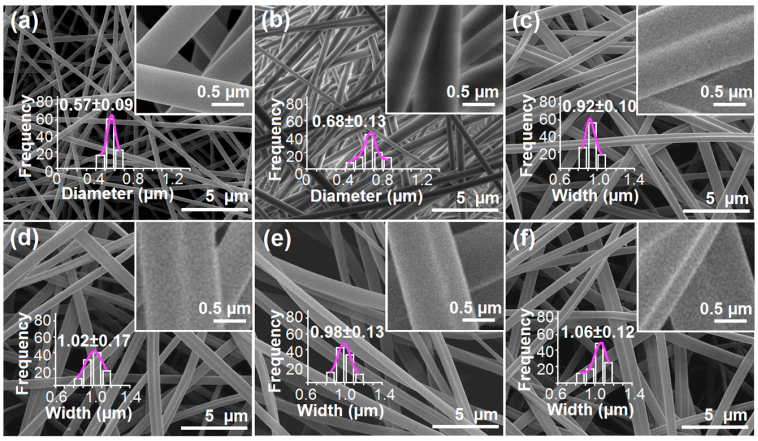

Fig. 2. FESEM images of the fibers, together with their size distributions: (a) F1 (drug-loaded PVP fibers); (b) F2 (drug-loaded EC fibers); and the Janus PVP/EC/KET fibers (c) F3; (d) F4; (e) F5; (f) F6.

TEM images of F3, F4, F5 and F6 are displayed in Fig. 3a to Fig. 3d. Two different sides to the fibers can again be discerned, with the larger and slightly darker side being the EC compartment. In the TEM image of F3 (Fig. 3a), there is a central region with a lower contrast level, suggesting a concave topography. F4 (Fig. 3b)

shows forks resulting from separation of the two sides of the fiber.

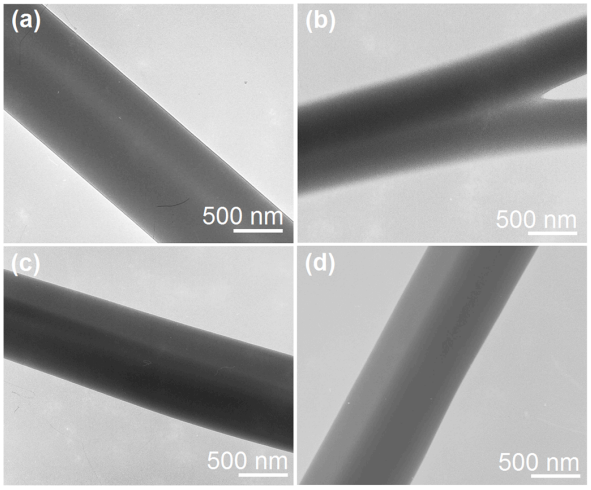

Fig. 3. TEM images of (a) F3; (b) F4; (c) F5; (d) F6.

3.3. *In vitro* dissolution tests

All the fibers are polymeric composites with KET present in an amorphous state due to the the existence of hydrogen bonding and hydrophobic interactions between the drug and its carrier (see the Supplementary Information, Figs. S2 to S4). In the *in vitro* dissolution tests, the monolithic PVP fibers F1 provide a very fast drug release profile, freeing all the loaded drug within one minute (Fig. 4a and Table 2). This can be attributed to the large surface area and small diameter of the individual nanofibers, the porous 3D web structures of the fiber mats, the highly hydrophilic and fast-dissolving nature of PVP, and the amorphous state of KET in the fibers. In contrast, the F2 (EC) fibers give a sustained release profile (Fig. 4a and Table 2), with release of 10.7% and 33.4% in the first minute and first hour, respectively. After 24 h, 82.5% of the embedded KET has been released. The Janus fibers F3 to F6 result in biphasic drug release profiles, with a portion of the embedded drug being released rapidly into the dissolution medium with the dissolution of the PVP side of the fibers.

328 Subsequently, the EC side of the fibers leads to sustained release of KET (Fig. 4a and
329 Table 2). The addition of small amounts of PVP K10 to the EC side of the fibers
330 permits the release in the second, sustained, phase to be tuned. An increase in PVP
331 K10 content causes the release rate and the percentage released after 24 h to increase
332 correspondingly (Fig. 4b and Table 2). The F6 fibers, with 16.1% w/w PVP K10 in
333 the EC side, released all the incorporated drug within 16 h.

334 The second phase of the *in vitro* dissolution data (up to 16 h) was analyzed using
335 the zero-order equation and Peppas equations:

336 Zero-order equation [31]: $Q_z = a + r\,t_z$

337 *(*where Q_z is the release percentage, t_z is the time, a is a constant and r is the release
338 rate).

339 Peppas equation: $Q_p = kt_p^n$

340 *(*where Q_p is the release percentage, t_p is the time, k is a constant and n is an exponent
341 that indicates the release mechanism).

342 The results of this analysis are shown in Table 2. Release from the EC side of the
343 fibers appears to follow a typical Fickian diffusion mechanism; the values of the
344 exponent n are all smaller than 0.45. The zero-order equation provides a simple way
345 to compare the release rate (r) from the EC side of the different Janus fibers. As the
346 content of PVP K10 (C) in the EC side was increased from 0% to 3.7%, 7.1% and
347 16.1% w/w, the r values increased correspondingly from 2.16, to 2.31, 2.38 and 2.65
348 h^{-1}, respectively. A linear relationship can be established: $r = 2.1756+0.0297C$
349 (R=0.9964; Fig. 4b). This demonstrates that the drug release rate from the EC matrix

can be easily manipulated through doping with hydrophilic PVP K10.

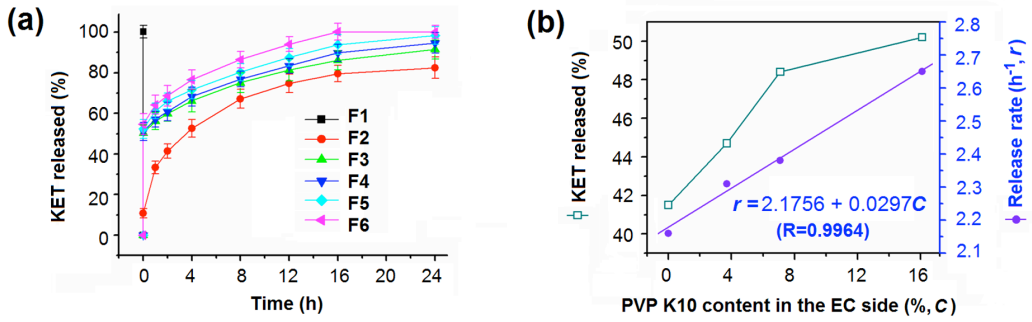

Fig. 4. The release of KET from the electrospun nanofibers: (a) The *in vitro* KET release profiles from the six fibers; **(b)** the variation of the release percentage and rate in the second phase as a function of the PVP K10 content in the EC side of the fibers.

Table 2. Data on the release of KET from the drug-loaded fibers [a,b] (n=6).

Fiber	First phase (1 min, %)	Rel after 24 h (%)	Second phase of release		
			Rel[c] (%)	Regressed equation (to 16h)	
				Peppas	Zero-order
F1	100±2.8	--	--	--	--
F2	10.7±2.2	82.5±5.3	--	$Q_{p2}=33.46t_{p2}^{0.3252}$ ($R_{p2}=0.9982$)	--
F3	50.4±3.9	91.5±4.7	41.1 (41.5)	$Q_{p3}=54.61t_{p3}^{0.1576}$ ($R_{p3}=0.9921$)	$Q_{z3}=54.62+2.16t_{z3}$ ($R_{z3}=0.9773$)
F4	51.4±4.4	94.7±5.1	43.3 (44.7)	$Q_{p4}=55.54t_{p4}^{0.1621}$ ($R_{p4}=0.9932$)	$Q_{z4}=55.44+2.31\ t_{z4}$ ($R_{z4}=0.9798$)
F5	52.3±4.7	98.4±4.3	46.1 (48.4)	$Q_{p5}=59.78t_{p5}^{0.1525}$ ($R_{p5}=0.9899$)	$Q_{z5}=58.71+2.38\ t_{z5}$ ($R_{z5}=0.9710$)
F6	54.7±5.2	100.2±3.2	45.5 (50.2)	$Q_{p6}=62.53t_{p6}^{0.1624}$ ($R_{p6}=0.9927$)	$Q_{z6}=61.61+2.65\ t_{z6}$ ($R_{z6}=0.9693$)

[a] The burst release in the first minute is defined as the first phase, and the data between the first minute and 16h were used to determine the drug release equations.

[b] Abbreviations: Q_{p2}, t_{p2}, and R_{p2} refer to the release percentage, time and correlation coefficient calculated with the Peppas equation for F2. Q_{z2}, t_{z2}, and R_{z2} are the release percentage, time and correlation coefficient determined with the zero-order equation for nanofibers F2. Quantities are defined similarly for the other fibers; the numerical subscript gives the identity of the fiber sample under consideration.

[c] The percentage released in the second phase was calculated by subtracting the percentage of drug released in the first stage from the release percentage after 24 h. The values in brackets represent the percentage of the total

amount of drug release which came from the EC sides (i.e. the drug content released after 24 h minus 50%, the amount of drug in the PVP side of the fibres).

3.4. Drug release mechanism

To investigate the drug release mechanism, samples were recovered from the dissolution apparatus after 24h and dried in air. The SEM results, shown in Fig. 5a to 5d, show the morphologies of the EC side of the fibers (the PVP side dissolves completely in a few seconds). Although the overall Janus fibers did not appear to be affected by the addition of PVP K10 to the EC side, the size of the fibers recovered after 24h of dissolution appears to decrease with an increase of PVP K10 content, and they have increasingly curved morphologies (see the Supplementary Information, Fig. S5). The remnant nanofibers had rough and wrinkled surfaces, displaying holes and grooves; larger PVP K10 contents appear to promote more of these features.

Fig. 5. FESEM images of the fibers remaining after 24h of dissolution and the proposed drug release mechanism. (a) to (d) show the remains of fibers F3 to F6 respectively; (e) is a schematic diagram explaining the mechanism of drug release from the Janus fibers.

A potential mechanism underlying the biphasic release profile is given in Fig. 5e.

After encountering water, the PVP K60 side of the Janus fibers will dissolve very rapidly and immediately free all the drug it contains. The remaining EC side provides the sustained release phase. When there is no PVP K10 in the EC side, as the case of F3, water diffuses into the EC matrix very slowly. KET is a poorly water soluble drug, and thus the dissolution of KET and its diffusion from the interior of the fibers to the dissolution medium proceed very slowly. Because EC is totally insoluble in water, it is inevitable that a certain amount of KET will remain trapped in the fibers and cannot be released even after 24 h.

The PVP K10 doped in the EC side of the fibers is highly soluble in water, and thus will dissolve rapidly on encountering water. As it does so, it will generate holes and pores in the EC matrix. The presence of increased amounts of PVP K10 will enhance this effect. The pores formed after dissolution of PVP K10 will facilitate the diffusion of water to the interior of the EC matrix, and of KET molecules into the dissolution media. This in turn increases the drug release rate and amount in the second phase of release. Further increases of PVP K10 content will yield interconnected pores, further aiding the movement of water into and drug out of the inside of the fibers, as is the case for the Janus fibers F6 (Fig. 5d).

As a counterpart of the core-shell structure, the Janus structure can be exploited to develop a wide variety of functional and multi-functional nanomaterials [32]. The side-by-side electrospinning process reported here is easy to undertake, and our results should expand the possibilities for exploiting electrospinning to fabricate novel functional nanocomposites with Janus morphology. There are many possibilities for

425 the use of such materials in developing new biomedical materials, in addition to the
426 tunable biphasic release systems reported here. For example, the fibers could be
427 exploited to develop systems permitting the controlled release of multiple drugs for a
428 combined therapy, or for new wound dressings with one side providing adhesive and
429 anti-inflammatory functions and the other providing sustained release of the active
430 ingredients required for wound healing. By collecting Janus nanofibers in an aligned
431 [33] or layer-by-layer fashion [34] additional strategies can be conceived for
432 generating novel structures and building new structure-property-activity relationships.
433 Furthermore, coaxial electrospinning allows the field of materials which can be
434 electrospun to be broadened considerably, as often electrospinning can be achieved
435 with only one of the two working fluids being electrospinnable on its own [35].
436 Similarly, it might be possible to implement side-by-side electrospinning using one
437 spinnable and one unspinnable fluid. This possibility is being studied at present. Much
438 work has been undertaken to explore the scalability of single-fluid electrospinning
439 [36,37], with very promising results. Hence, the generation of Janus fibers on a large
440 scale should be eminently possible, and the novel nanoscale DDS which can be
441 generated using such fibers have the real possibility for clinical translation [38].

442 ## 4. Conclusion

443 In summary, here we developed a Teflon-coated spinneret which could be used for
444 highly effective and stable side-by-side electrospinning. The use of a Teflon coating
445 can effectively prevent the separation of the two working fluids seen when attempting
446 electrospinning with no coating. A series of medicated Janus fibers was successfully

fabricated; these had two distinct sides respectively made of poly(vinylpyrrolidone) (PVP) K60 and ethyl cellulose (EC), loaded with ketoprofen (KET) as a model active ingredient. PVP K10 was added to the EC side of the fibers in some cases to act as a porogen. Electron microscopy images clearly demonstrated that integrated Janus fiber structures were produced, in which the KET was found to be amorphously distributed. *In vitro* dissolution tests demonstrated that all the Janus fibers were able to provide a biphasic controlled release profile, with an initial burst followed a slower and sustained release phase. By varying the amount of PVP K10 doped in the EC side of the fibers, the release rate and total release percentage can be precisely tuned. Our results proffer a platform for designing novel drug delivery systems that can provide a tunable release profile designed to complement natural biological rhythms for maximum therapeutic effects.

Acknowledgments

This work was supported by the National Science Foundation of China (Nos. 51373101 and 51373100), the China NSFC/UK Royal Society cost share international exchanges scheme (No. 51411130128/IE131748) and the Hujiang Foundation of China (B14006).

References

[1] S. Agarwal, A. Greiner, J.H. Wendorff, Prog. Polym. Sci. 38 (2013) 963.

[2] P. Tonglairoum, T. Ngawhirunpat, T. Rojanarata, R. Kaomongkolgit, P. Opanasopit, Colloids Surf. B 126 (2015) 18.

[3] W. Liu, Z. Wu, Y. Wang, Z. Tang, J. Du, L. Yuan, D. Li, H. Chen, J. Mater. Chem. B 2 (2014) 4272.

[4] Z. Tang, D. Li, X. Liu, Z. Wu, W. Liu, J.L. Brash, H. Chen, Polym. Chem. 4 (2013) 1583.

[5] W. Yang, J. Fu, D. Wang, T. Wang, H. Wang, S. Jin, N. He, J. Biomed. Nanotechnol. 6 (2010) 254.

[6] X. Ji, T. Wang, L. Guo, J. Xiao, Z. Li, L. Zhang, Y. Deng, N. He, J. Biomed. Nanotechnol. 9 (2013) 417.

[7] Z. Aytac, S.Y. Dogan, T. Tekinay, T. Uyar, Colloids Surf. B 120 (2014) 125.

[8] Q. Shi, Q. Fan, W. Ye, J. Hou, S.C. Wong, X. Xu, J. Yin, Colloids Surf. B 125 (2015) 28.

[9] T. Wang, X. Ji, L. Jin, Z. Feng, J. Wu, J. Zheng, H. Wang, Z.W. Xu, L. Guo, N. He, ACS Appl. Mater. Interfaces 5 (2013) 3757.

[10] X. Ji, W. Yang, T. Wang, C. Mao, L. Guo, J. Xiao, N. He, J. Biomed. Nanotechnol. 9 (2013) 1672.

[11] W. Wang, Z. Li, T. Jiang, Z. Zhao, Y. Li, Z. Wang, C. Wang, ACS Appl. Mater. Interfaces 4 (2012) 6080.

[12] A.V. Bazilevsky, A.L. Yarin, C.M. Megaridis, Langmuir 23 (2007) 2311.

[13] X. Xu, X. Zhuang, X. Chen, X. Wang, L. Yang, X. Jing, Macromol. Rapid Commun. 27 (2006) 1637.

[14] D.G. Yu, X. Li, X. Wang, J. Yang, S.W.A. Bligh, G. Williams, ACS Appl. Mater. Interfaces 7 (2015) 18891.

[15] Z. Ahmad, H.B. Zhang, U. Farook, M. Edirisinghe, E. Stride, P. Colombo, J. R. Soc. Interfaces 5 (2008) 1255.

[16] W. Chen, Z. Ma, X. Pan, Z. Hu, G. Dong, S. Zhou, M. Peng, J. Qiu, J. Am. Ceram. Soc. 97 (2014) 1944-1951.

[17] S. Jiang, S. Granick, (Ed.): Janus particle synthesis, self-assembly and applications (RSC) 2012, p5-p15.

[18] J. Hu, S. Zhou, Y. Sun, X. Fang, L. Wu, Chem. Soc. Rev. 41 (2012) 4356.

[19] A. Walther, A. H. E. Müller, Chem. Rev. 113 (2013) 5194.

[20] P. Gupta, G. L. Wilkes, Polymer 44 (2003) 6353.

[21] G. Chen, Y. Xu, D.G. Yu, D.F. Zhang, N.P. Chatterton, K.N. White, Chem. Commun. 51 (2015) 4623.

[22] J.D. Starr, J.S. Andrew, Chem. Comm. 49 (2013) 4151.

[23] J.D. Starr, M. A.K. Budi, J.S. Andrew, J. Am. Ceram. Soc. 98 (2015) 12.

[24] D.G. Yu, X. Wang, X.Y. Li, W. Chian, Y. Li, Y.Z. Liao, Acta Biomater. 9 (2013) 5665.

[25] D.G. Yu, F. Liu, L. Cui, Z.P. Liu, X. Wang, S.W.A. Bligh, RSC Adv. 3 (2013) 17775.

[26] B. Song, C. Wu, J. Chang, Acta Biomater. 8 (2012) 1901.

[27] L.Y. Huang, C. Branford-White, X.X. Shen, D.G. Yu, L.M. Zhu, Int. J. Pharm. 436 (2012) 88.

[28] W. Qian, D.G. Yu, Y. Li, Y.Z. Liao, X. Wang, L. Wang, Int. J. Mol. Sci. 15 (2014) 774.

[29] P.K. Gupta, J.R. Robinson, Oral Controlled-release delivery. In: A. Kydonieus, (Ed.), Treatise on controlled drug delivery. Marcel Dekker, New York, 1992,

pp.255-313.

[30] C. Li, Z.H. Wang, D.G. Yu. Colloids Surf. B 114 (2014) 404.

[31] N.A. Peppas, Pharm Acta Hel 60 (1985)110.

[32] S. Venkataraman, J.L. Hedrick, Z.Y. Ong, C. Yang, P.L. Rachel Ee, P.T. Hammond, Y.Y. Yang. Adv. Drug Del. Rev. 63 (2011) 1228.

[33] J. Xie, W. Liu, M.R. MacEwan, P.C. Bridgman, Y. Xia, ACS Nano 8 (2014) 1878.

[34] B. Zhou, Y. Li, H. Deng, Y. Hu, B. Li, Colloids Surf. B 116 (2014) 432.

[35] Y.H. Wu, D.G. Yu, X.Y. Li, A.H. Diao, U.E. Illangakoon, G.R. Williams, J. Mater. Sci. 50 (2015) 3604.

[36] F. Yener, O. Jirsak, J. Nanomater. 2012 (2012) 839317.

[37] Z.K. Nagy, A. Balogh, B. Démuth, H. Pataki, T. Vigh, B. Szabó, K. Molnár, B.T. Schmidt, P. Horák, G. Marosi, G. Verreck, I. Van Assche, M.E. Brewster, Int. J. Pharm. 480 (2015) 137.

[38] B. Démuth, Z.K. Nagy, A. Balogh, T. Vigh, G. Marosi, G. Verreck, I. Van Assche, M.E. Brewster, Inter. J. Pharm. 486 (2015) 268.

Captions of Tables and Figures

Table 1. Details of the electrospinning processes and the resultant product.

Table 2. Data on the release of KET from the drug-loaded fibers [a,b] (n=6).

Fig. 1. The side-by-side electrospinning process: (a) The experimental apparatus (inset: the connection of the side-by-side spinneret with the working fluids and power supply); (b) a photograph of a typical side-by-side electrospinning process with the Teflon-coated spinneret; (c) a Janus Taylor cone formed with the Teflon-coated spinneret; (d) The fiber mat from side-by-side electrospinning with the uncoated side-by-side spinneret; (e) the separation of fluids when using the uncoated spinneret; (f) an illustration of the role played by the Teflon coating: A - the separation of fluids arising from repulsive forces F_t (between the two Taylor cones), F_s (between the two straight fluid jets) and F_c (between the two coils); and B - the formation of an integrated Janus Taylor cone with the Teflon coating.

Fig. 2. FESEM images of the fibers, together with their size distributions: (a) F1 (drug-loaded PVP fibers); (b) F2 (drug-loaded EC fibers); and the Janus PVP/EC/KET fibers (c) F3; (d) F4; (e) F5; (f) F6.

Fig. 3. TEM images of (a) F3; (b) F4; (c) F5; (d) F6.

Fig. 4. The release of KET from the electrospun nanofibers: (a) The *in vitro* KET release profiles from the six fibers; (b) the variation of the release percentage and rate in the second phase as a function of the PVP K10 content in the EC side of the fibers.

Fig. 5. FESEM images of the fibers remaining after 24h of dissolution and the proposed drug release mechanism. (a) to (d) show the remains of fibers F3 to F6 respectively; (e) is a schematic diagram explaining the mechanism of drug release from the Janus fibers.